

# Observing the adsorption process of friction modifier additives by combination of quartz crystal microbalance (QCM-D) and confocal laser scanning microscopy (CLSM)

*Jennifer Eickworth<sup>1</sup>, Martin Dienwiebel<sup>1,2</sup>, Thomas Rühle<sup>3</sup>, Patrick Wilke<sup>3</sup>*

1 Fraunhofer IWM MikroTribologie Centrum, Wöhlerstraße 11, 79108 Freiburg, Germany

2 Karlsruher Institut für Technologie KIT, Kaiserstraße 12, 76131 Karlsruhe, Germany

3 BASF SE, Carl-Bosch-Straße 38, 67036, Ludwigshafen, Germany

## KEYWORDS

lubricants, friction modifier, QCM-D, CLSM, deposition

## ABSTRACT

Friction modifier additive technologies play a crucial role in minimizing friction and wear of lubricated tribological systems. Present efforts to improve the energy efficiency and new

regulations require a fundamental understanding of the adsorption processes. Therefore *in-situ* and oil compatible methods are needed.

This work combines the in-situ measurement of friction modifier additives deposition onto a surface and the resulting viscoelastic properties (using a quartz crystal microbalance with dissipation, QCM-D) with the imaging of the deposition process employing a fluorescence confocal laser scanning microscope (CLSM). This approach enabled us to for the first time to observe the deposition *in-situ*.

Contrary to the common assumption present for almost 100 years that friction modifiers form monolayers, our CLSM-study shows that friction modifiers can also form droplets in the mineral base oil and subsequently stay in the shape of a droplet after deposition on the Fe<sub>2</sub>O<sub>3</sub> surface. The adsorbed droplets have diameters between  $< 1 \mu\text{m}$  and  $127 \mu\text{m}$ . Small droplets are not mobile after deposition, but droplets with a certain diameter become mobile and move along the surface to merge with other mostly smaller droplets. We also find that droplets in solution prefer coalescence with already adsorbed droplets over deposition. From distribution and size of the adsorbed droplets the adsorbed amount is calculated and correlated with the values found with QCM-D.

Hence, the combination with QCM-D the ongoing processes can be described quantitative and qualitative to give completely new insights in the deposition processes.

## INTRODUCTION

The main classes of friction modifiers can be roughly divided into organic friction modifiers (OFM), functionalized polymers, soluble organo-molybdenum additives and dispersed nanoparticles [1]. Besides fatty acids, OFM's can comprise of carboxylates, alcohols, imides, borates, phosphorus compounds, ionic liquids, amides and amines[2]. The adsorption mechanism and mode of action of fatty acids was in the focus of numerous studies during the last century (e.g. [3-8]) and the friction reduction is often explained using the boundary lubrication model that goes back to Hardy in 1922 [9]. The ongoing trend towards low-viscosity oils in order to reduce liquid friction losses increases the requirements especially for friction modifier additives, as friction must remain low even in the mixed lubrication regime. Moreover, as fatty acids can be corrosive and can cause damage, amines and their derivatives are a promising alternative. Therefore more recently, research on OFM has gained new interest and the adsorption behavior of amines has been reported in literature as well, but not to such extent as fatty acids. This lack of knowledge and more stringent environmental guidelines motivated us to seek a better understanding of the adsorption of amine based friction modifiers.

*Benitz et al.* [10] studied the formation of self-assembled monolayers of octadecylamine on mica surfaces using chloroform as hydrophobic solvent with an atomic force microscope (AFM). The mica surfaces were immersed in 15 mM solutions (0.4 wt.%) at RT, removed and dried with N<sub>2</sub>. Octadecylamine forms 0.3 μm to 0.5 μm wide and 1.6 nm high islands on the mica surface. Friction maps showed that the friction is reduced in the area of the islands. Ripening of the formed islands in air lead to larger islands, which indicates a certain mobility of the islands. Longer immersion times produce much more but smaller islands [10].

*Zhu et al. [11]* used a surface forces apparatus (SFA) modified for oscillatory shear tests to study the nano-rheological properties of hexadecylamine solved in tetradecane. The “hard-wall film thickness” was determined to be 4.7 nm (for 0.1 wt.% solutions) resulting from hexadecylamine molecules adsorbed at both mica surfaces (1.8 nm each) and 2 to 3 layers of randomly oriented molecules in between. In the oscillatory shear tests pure tetradecane showed a stick-slip transition and a limiting shear stress of 6.5 Pa, whereas the addition of 0.1 wt.% hexadecylamine did not show stick-slip and did reduce the limiting shear stress to 5.4 Pa.

The investigations of *Wood et al. [12]* and *Doig and Camp [13]* were more application-oriented as they used iron oxide surfaces. *Wood et al.* studied the hexadecylamine adsorption from hexadecane using polarized neutron reflectometry (PNR) and X-ray photoelectron spectroscopy (XPS) on an iron oxide layer (mixture of  $\text{Fe}_2\text{O}_3$  and  $\text{Fe}_3\text{O}_4$ ). For low amine concentrations, 1 and  $4 \times 10^{-4}$  mol/dm<sup>3</sup> (0.02 and 0.1 wt.%) the layer thickness was found to be 1.6 nm. Higher concentrations, 1 and  $4 \times 10^{-3}$  mol/dm<sup>3</sup> (0.24 and 0.97 wt.%) slightly increase the film thickness to 2 nm. As the length of an extended hexadecylamine molecule is 2.15 nm [14] the adsorbed molecules are supposed to be tilted by 42° (for 1.6 nm thickness) and 22° (for 2 nm thickness). For XPS analysis an iron oxide surface was treated with 1.03 wt.% solution of hexadecylamine in hexadecane. The N1s emission line shows three peaks. The main peak results from the reaction of the amine with the surface and *Wood et al.* expect the nitrogen to donate an electron to the iron oxide surface and chemisorb, which means that the polar headgroups are located at the iron-oil interface (classic thin film brush model for friction modifiers) [11]. *Doig and Camp* performed MD simulations under the same conditions as *Wood et.al*, to compare experimental and simulation data. The calculated values for the film thicknesses are in good agreement with the experimental data and were found to be 1.5 nm and 2 nm. From radial distribution functions

it was shown, that the positions of the headgroups are prescribed by the lattice of the iron oxide surface, but that the ordering strongly decreases with a larger distance from the surface [13].

Except the work of *Zhu et.al.*, all presented investigations are ex-situ studies. *Eriksson* [15] and *Nalam et al.*[16] performed *in-situ* studies using the quartz crystal microbalance (QCM) with stainless steel coated quartz sensors. *Eriksson* studied the adsorption of tertiary amine ethoxylate and primary oleyl amine from commercially available group III engine oil. The QCM tests were performed at 50 °C and a flow rate of 250  $\mu\text{l}/\text{min}$ . The amine ethoxylate adsorbs with 100  $\text{ng}/\text{cm}^2$  from a 1 wt.% solution and the oleyl amine with 27  $\text{ng}/\text{cm}^2$  from a 0.5 wt.% solution [15]. *Nalam et al.* found adsorbed amount in the same order of magnitude for a di-fatty amine (39  $\text{ng}/\text{cm}^2$ ), a charged di-fatty amine (40  $\text{ng}/\text{cm}^2$ ), a tri-fatty amine (46  $\text{ng}/\text{cm}^2$ ) and a branched tri-fatty amine (58  $\text{ng}/\text{cm}^2$ ) from 0.5 wt.% solutions in hexadecane. The corresponding layer thicknesses are in the range of 0.46 nm to 0.71 nm and the authors suggest the molecules to adsorb with a certain tilt angle or even parallel to the surface [16].

The presented research clearly shows the research gap when it comes to the combination of qualitative and quantitative studies. QCM is a powerful tool to investigate adsorbed amount, but does not provide information about the morphology of the adsorbent. All calculations to find film thicknesses are based on the model of monolayer adsorption, although the imaging of an adsorbed amine film with AFM showed island growth (cf. Ref. 10). Most of the research was performed using model fluids as solvents and friction modifiers.

This apparent predicament is in the center of our study, which is why we combined quantitative QCM measurements with qualitative fluorescence confocal laser scanning microscope (CLSM)

imaging, in order to investigate the deposition process of a commercially employed friction modifier from a group II mineral base oil.

## EXPERIMENTAL

### MATERIALS

We used a commercially available friction modifier (IRGALUBE® FE 1), which is an organic compound whose chemistry is broadly described in Ref. 17. We will abbreviate the additive as FA in the remainder of the paper. The relevant physical properties are given in Table 1. The head group can be a propyl group, an ester group or an alcohol group. The concentration of the FA was set to 1 wt.% for all measurements. As solvent a pure group II mineral base oil was used, abbreviated as BO. The mixture of BO and 1 wt.% FA is a non-stable emulsion. The FA forms droplets in BO, which coalesce and sediment due to the higher density of the FA compared to BO. As a non-polar reference oil a PAO 6 was used. higher density of the FA compared to BO.

Table 1. Physical properties of FA, BO and BO + 1 wt.% FA

	FA	BO	BO + 1 wt.% FA
kinematic viscosity [mm <sup>2</sup> /s]	290 (20 °C)	25.48 (55 °C)	25.94 (55°C)
density [g/cm <sup>3</sup> ]	0.97 (20 °C)	0.84 (55 °C)	0.84 (55°C)

As surfaces for the QCM-D experiments commercially available Fe<sub>2</sub>O<sub>3</sub>-coated 5 MHz quartz crystals with a roughness of 1.7 ± 0.1 nm (Biolin Scientific GmbH, Gothenburg, Sweden) were used.

## METHODS

### Quartz Crystal Microbalance with Dissipation (QCM-D)

The QCM measurements are performed using a QSense E4 (Biolin Scientific GmbH, Gothenburg, Sweden). The cell temperature is set to 55 °C and the oil is pumped through the cell using a peristaltic pump (Cole-Parmer GmbH, Wertheim, Germany). Each measurement starts with a non-polar reference oil to find the base line. After equilibrating the system the following sequence is used for rinsing: 30 min reference oil, 30 min BO, 60 min BO + 1 wt.% FA, 30 min BO, 30 min reference oil. The flow rate is 130 µl/min<sup>1</sup>. For the present work only the rinsing steps 30 min BO, 60 min BO + 1 wt.% FA, 30 min BO are relevant, therefore the results are normalized to the BO as base line ( $\Delta f$  and  $\Delta D$  are set to zero).

The signals used from the QCM-d are the frequency changes  $\Delta f$  and the dissipation shifts  $\Delta D$ .  $\Delta f$  can be converted in a mass change  $\Delta m$  using the Sauerbrey equation [18]:

$$\Delta m = -C \cdot \Delta f \quad (1)$$

The proportionality constant or mass sensitivity constant  $C$  can be calculated from the thickness and intrinsic parameters of the crystal. For 5 MHz AT-cut quartz crystals the Sauerbrey constant is  $C = 17.7 \text{ ng}/(\text{cm}^2 \cdot \text{Hz})$  (for details and parameters see e.g. Ref. 19). The calculation of

---

<sup>1</sup> The used peristaltic pump Ismatec IPC (Cole-Parmer GmbH, Wertheim, Germany) is set to 200µl/min, calibrated for water.

adsorbed masses using the Sauerbrey equation can only be regarded valid if the following conditions are fulfilled: (1) the adsorbed masses are small compared to the weight of quartz crystal:  $\frac{\Delta f}{f} \ll 1$  [19], (2) the adsorbed masses are distributed homogeneously on the surface, as the mass sensitivity is Gaussian-shaped and has its maximum in the center [20], and (3) the adsorbed masses form rigid, non-deformable films on the surface and therewith have small dissipation shifts:  $\Delta D \leq 1E - 6$  [19,21].

For the tested systems the 3<sup>rd</sup> condition is not fulfilled as  $\Delta D$  is much higher ( $\Delta D \approx 460 E - 6$ ).  $\Delta m$  calculated with the Sauerbrey equation is underestimated in this case. Nevertheless, the assumption can be made to calculate a generally understandable value, which is not absolute but can be compared relatively.

The oscillation of the quartz sensors has a decay length  $\delta$  into the immersed liquid that depends on the viscosity  $\vartheta_l$  and the density  $\rho_l$ . Specifically, the oscillation (angular frequency  $\omega$ ) decays with [19] in the  $z$ -direction, i.e. perpendicular to the surface:

$$\delta = \left( \frac{2 \cdot \vartheta_l}{\omega \cdot \rho_l} \right)^{0.5} \quad (2)$$

Thus, films with a thickness lower than the decay length are detected fully (finite thickness), whereas films with a larger film thickness than the decay length (semi-infinite thickness) can be detected partially [19]. The decay lengths for the measured liquids result from the given physical values and equation (2) to 1.28  $\mu\text{m}$  for BO and to 1.29  $\mu\text{m}$  BO + 1 wt.% FA.

### **Confocal Laser Scanning Microscopy (CLSM)**



For the CLSM measurements a *Leica SP5 DM6000 B* (Leica Microsystems GmbH, Wetzlar, Germany) with a *HC FLUOTAR L 25x/0.95 W VISIR* objective (Leica Microsystems GmbH, Wetzlar, Germany) was used. The SP5 is an upright microscope system with a lateral resolution of maximum 200 nm. For the experiments a flow cell with a geometry close to the QCM-D (true to scale replica) was used. The schematic of the measurement setup is depicted in Figure 1. The oil is pumped through the cell with a flow rate of approximately 140  $\mu\text{l}/\text{min}$ . The cell is first filled with BO to ensure the sealing and wetting of the  $\text{Fe}_2\text{O}_3$  surface. The  $\text{Fe}_2\text{O}_3$  surfaces are the same as in the QCM-D measurements but the quartzes need to be cut in smaller pieces to fit into the flow cell. After all preparations are completed, the quartzes were rinsed with BO + 1 wt.% FA. At the start of the experiment, the  $\text{Fe}_2\text{O}_3$  surface is brought into the focus of the microscope. The ongoing processes can be detected as a function of time in the xy-plane (side view) or xz-plane (top view).

## RESULTS AND DISCUSSION

### Quartz Crystal Microbalance with Dissipation (QCM-D)

Figure 2 shows the resonance frequency shift of the 5th overtone during the deposition of 1 wt.% FA from BO on  $\text{Fe}_2\text{O}_3$ . The shown result is the mean value of 7 measurements between 0 min and 120 min. With the injection of 1 wt.% FA the frequency drops by -1.5 Hz which indicates a mass increase of 27  $\text{ng}/\text{cm}^2$  (deposition). The results are in good accordance with the results from *Eriksson* [15] and *Nalam et al.* [16]. Interestingly, by changing the medium back to BO the frequency decreases again by -8.8 Hz which suggests another deposition step of 156  $\text{ng}/\text{cm}^2$ . Therefore, in total at the end of the test, 183  $\text{ng}/\text{cm}^2$  FA is adsorbed at the  $\text{Fe}_2\text{O}_3$  surface.

It has been shown that many organic friction modifiers form viscous boundary layers [1]. Therefore we first calculated a constant layer thickness under the assumption that the density of the adsorbed FA is the same as in the bulk material. The calculated thickness of this layer before rinsing with BO again is 0.27 nm and after rinsing it amounts to 1.88 nm. As the layer thicknesses are thinner than a monolayer would be, it is likely that FA is not adsorbed as a dense layer but grows as islands. Alternatively, a tilted configuration would be possible.

Figure 3 represents the dissipation shift for the deposition of 1 wt.% FA from BO on Fe<sub>2</sub>O<sub>3</sub>. Adding 1 wt.% FA leads to a drop in the dissipation shift which equilibrates after a few minutes to a negative dissipation shift of -0.7, which means that the adsorbent is slightly less viscoelastic than the BO. This could be the fact that BO forms a mostly fluid and exchangeable layer at the surface (no or little deposition) while the adsorbed FA is stronger attached to the surface (deposition). The rinsing step with BO increases the dissipation above the initial level by 2.3, which indicates a more viscoelastic behavior and one could initially speculate that the FA has been removed. However, in this case the mass should be decreasing. At this point it must be pointed out again that the dissipation of the pure base oil is already very high and the changes are comparatively small.

These results can therefore be summarized as follows. The addition of FA leads to an increase in mass and a decrease in viscoelasticity, whereas during the rinsing step with BO, the adsorbed mass and the viscoelasticity increase again. At this point, it is not possible to understand this result and a more realistic viscoelastic model needs to be employed [22] which would require knowledge of the surface coverage of the adsorbed FA layer. This however is not possible without an additional experimental method, as the QCM-D provides no information about the structure of the adsorbed FA film.

## Confocal Laser Scanning Microscopy (CLSM)

### Rinsing step BO to BO + 1 wt.% FA

Figure 4 depicts the approach and deposition process of a FA droplet emulsified in BO onto the  $\text{Fe}_2\text{O}_3$  surface in the  $xz$ -plane. The grey contrast is due to the reflection signal of the  $\text{Fe}_2\text{O}_3$  surface at 405 nm. The BO does not fluoresce and FA does show fluorescence at 488 nm and is shown in orange. The representative series of images show a droplet with a diameter of approximately 21  $\mu\text{m}$  approaching the  $\text{Fe}_2\text{O}_3$  surface. Within 37 seconds, the drop reduces its distance from the surface before then adsorbing and spreading slightly. The adsorbed droplets appear to be stable afterwards. However, the resolution of the CLSM method does not allow to detect if there is a thinner FA layer between the adsorbed droplets.

Figure 5 is a time series that shows the merging process of two FA droplets in  $xz$ -plane. This series was taken during the rinsing with BO + 1 wt.% FA and was observed parallel to the deposition processes shown in Figure 4. A droplet with a diameter of approximately 25  $\mu\text{m}$  is approaching the surface as seen already in Figure 4. This time the droplet does not adsorb at the  $\text{Fe}_2\text{O}_3$  surface but coalesces with a larger drop (diameter approximately 44  $\mu\text{m}$ ) already adsorbed at the surface. Since the conditions for deposition and coalescence have been the same and the coalescence has occurred, it can be assumed that this state is preferred in order to reduce the surface energy.

Figure 6 shows the deposition and merging processes of FA droplets in the xy-plane (top view). The greyish background is the  $\text{Fe}_2\text{O}_3$  surface and the orange droplets are again FA, fluorescent at 488 nm. During the first 4 min a few small droplets (diameters between 0.9  $\mu\text{m}$  and 23  $\mu\text{m}$ ) adsorb at the  $\text{Fe}_2\text{O}_3$  surface (Figure 6a-c). At 05:47 min in the lower right corner a larger drop appears (Figure 6 d). This droplet is mobile on the surface, but does not desorb. In the next minutes it moves along the surface (Figure 6e-f). At 13:05 min it merges with an also adsorbed smaller droplet (Figure 6g). We assume that droplets become mobile, if they reach a certain volume. They move along the surface and merge with other (mostly smaller) droplets.

On the basis of simple geometric considerations, the CLSM-images can be used to approximate the measured mass by QCM-D (Figure 7). For droplets with a radius larger than the decay length (cf. formula 2) the cylindrical volume  $V_{\text{cyl}}$  within the decay length is calculated and multiplied with the density of FA to find the theoretical QCM-D weight per drop  $m_{\text{CLSM}}$ . Droplets with a radius smaller than the decay length are taken into account with their total half-spherical volume  $V_{\text{sph}}$  (Figure 7). By adding up the weight of all droplets within the area  $400 \times 400 \mu\text{m}^2$  and recalculated the value to  $\text{ng}/\text{cm}^2$  the values can be compared with the mass shifts found with QCM-D. The histogram of the radii of the droplets for the time steps 03:00 min and 15:52 min of the image series shown in Figure 6 are given in Figure 8.

After rinsing the  $\text{Fe}_2\text{O}_3$  surface with BO + 1 wt.% FA for 3:00 min  $5.3 \text{ ng}/\text{cm}^2$  and after 15:52 min  $9.3 \text{ ng}/\text{cm}^2$  are adsorbed, which corresponds to a surface coverage of 0.4 % respectively 1.0 %. The mass values are both lower than the QCM-D value of  $27 \text{ ng}/\text{cm}^2$ , but are of the same order of magnitude. Unfortunately, with CLSM only a small area is investigated (which is a compromise between resolution and content of information). The area shown in Figure 6 appears to be an area with low droplet concentration.

From the dissipation shift in the QCM-D measurements (Figure 3) it is known that there is a drop directly after changing the medium from BO to BO + 1 wt.% FA. The adsorbing, mostly small droplets decrease the dissipation, so they are less viscoelastic than the initial BO environment. These findings are not intuitive, since one would assume that the droplets increase the viscoelasticity, as they are liquid and partially mobile. After a few minutes the dissipation shift stabilizes at a negative value of -0.7. From the histograms in Figure 8 one can conclude that the number of small droplets is shrinking at the expense of the large ones, which would indicate, that bigger drops are more viscoelastic than smaller ones.

### **Rinsing step BO + 1 wt.% FA to BO**

Figure 9 depicts a series of images when rinsing the Fe<sub>2</sub>O<sub>3</sub> surface with BO again, after rinsing with BO + 1 wt.% FA, in xy-plane. In the initial state, so during rinsing with BO + 1 wt.% FA, 5 bigger droplets (diameters between 88 μm and 127 μm) and a few smaller one (diameters < 1 μm) are adsorbed on the surface, which correspond to a surface coverage of 5.9 %. Due to rinsing with BO the amount of adsorbed FA droplets increase. In addition to the droplets already present in the initial state, there are now a higher number of smaller droplets (diameters < 1 μm) on the surface and the surface coverage increases to 6.6 %.

Using the same approach to calculate the theoretical masses from the CLSM as described above (compare Figure 7) for the initial state at time 1:32 min we obtain 73.3 ng/cm<sup>2</sup>. This value now is higher than the value found with QCM-D (27 ng/cm<sup>2</sup>), which can be due to two reasons: (1) the FA droplets are distributed non-homogenous on the Fe<sub>2</sub>O<sub>3</sub> surface and the results strongly depend on the investigated area and/or (2) the investigated area is representative and the QCM-D masses are underestimated. To investigate this in more detail further measurements at different

positions need to be done to find a statically validated distribution pattern and therewith a valid theoretical QCM-D weight. In this work only two areas were investigated, which the masses 9.3 ng/cm<sup>2</sup> and 73.3 ng/cm<sup>2</sup>. The mean value of both areas under the same conditions is 41.3 ng/cm<sup>2</sup> with a standard deviation of 32 ng/cm<sup>2</sup>. The QCM-D mass (27 ng/cm<sup>2</sup>) is therewith within the standard deviation.

At 3:10 min, after rinsing with BO for another 2 min, the CLSM-mass increases to 82.2 ng/cm<sup>2</sup>. With QCM-D the mass for this state is 183 ng/cm<sup>2</sup>.

The dissipation shift for the change from BO + 1 wt.% FA to BO was found to be 2.3 (Figure 3). The additional deposition of droplets thus not only results in an increase in mass, but also increase the viscoelasticity. The histograms in Figure 10 show that mostly small droplets with a radius < 5 μm additionally adsorb. Especially the number of droplets smaller than the decay length increases. The results found for the rinsing step with BO + 1 wt.% FA (described above) showed, that smaller drops are less viscoelastic than bigger ones. Here it turns out that a larger amount of smaller drop, especially smaller than the decay length are more viscoelastic than less bigger drops (compare the histogram in Figure 10). It seems that the number, the distribution and the size of the droplets and their interrelations are necessary to describe the dissipation shifts found with QCM-D.

A possible explanation for the additional deposition during rinsing with BO and therewith rinsing the Fe<sub>2</sub>O<sub>3</sub> surface with a less concentrated emulsion, we consider the solubility of FA in BO. During the rinsing process, adsorbed droplets could be released from the tubes and walls of the cell and adsorb on the Fe<sub>2</sub>O<sub>3</sub> surface instead. Additionally, rinsing might lead to a more

turbulent flow in the cell which leads to smaller droplets. As a result, more mass is detected by the QCM-D.

## CONCLUSIONS

Using QCM-D the frequency shift was measured and the corresponding mass was calculated using the Sauerbrey equation. It was found that the adsorbent, which is basically FA, adsorbs with 27 ng/cm<sup>2</sup>. As the resulting layer thickness of 0.27 nm is less than a monolayer, island growth can be assumed. Indeed CLSM measurements surprisingly show that the additive forms droplets in the base oil which stick onto the Fe<sub>2</sub>O<sub>3</sub> surface which contradicts the common assumption that friction modifiers form dense films. By recording CLSM videos it was for the first time possible to observe the deposition of FA droplets from BO on Fe<sub>2</sub>O<sub>3</sub> surfaces in-situ. The adsorbed FA droplets have radii varying between 0.4 μm and 14.5 μm. By adding up the weight of all droplets within the measurement area 400 x 400 μm<sup>2</sup> and recalculated the value to ng/cm<sup>2</sup> the values were compared with the mass shifts found with QCM-D. The mean value of both areas rinsed with BO + 1 wt.% is 41.3 ng/cm<sup>2</sup> with a standard deviation of 32 ng/cm<sup>2</sup>. Unfortunately, the standard deviation is very high, which results from the low number of random sampling and the fact that the FA droplets are non-homogeneously distributed on the Fe<sub>2</sub>O<sub>3</sub> surface and thus the results strongly depend on the investigated area. Nevertheless, the values are at the same order of magnitude and are reasonable considering the error. The correlation of the CLSM results and the dissipation shift found with QCM-D is not intuitive. The deposition of FA droplets decreases the viscoelasticity, even though the droplets are liquid and partially mobile. Finally, it is important to realize that the number, the distribution and the size of the droplets and their interrelations are relevant parameters to describe the dissipation shifts found with QCM-D alone. For this reason the combination of CLSM and QCM-D can be very valuable.

Another interesting observation of the FA was found during the rinsing step with BO + 1 wt.% FA. Parallel to deposition processes, merging of droplets was observed. If the conditions for deposition and coalescence are the same, coalescence occurs. This indicates that FA prefers the state of an emulsion not only over the solution in BO but also over deposition on Fe<sub>2</sub>O<sub>3</sub> surface. If droplets deposit on the surface they are not mobile until they reach a certain volume. Larger droplets are mobile and move along the surface and merge with other (mostly smaller) droplets.

Rinsing the Fe<sub>2</sub>O<sub>3</sub> surface with already adsorbed FA droplets with BO again, basically diluting the emulsion, interestingly leads to a second deposition step. With QCM-D the additionally adsorbed mass was found to be 156 ng/cm<sup>2</sup>. As a result at the end of the test, 183 ng/cm<sup>2</sup> FA is adsorbed at the Fe<sub>2</sub>O<sub>3</sub> surface. With CLSM we could not reproduce this phenomenon quantitatively, as the additionally amount adsorbed in the investigated area was only 10 ng/cm<sup>2</sup>, probably due to the higher amount before starting to rinse with BO again. Qualitatively, the additional deposition was confirmed by CLSM as the number of mainly smaller droplets increases during rinsing with BO.

## **FIGURES**



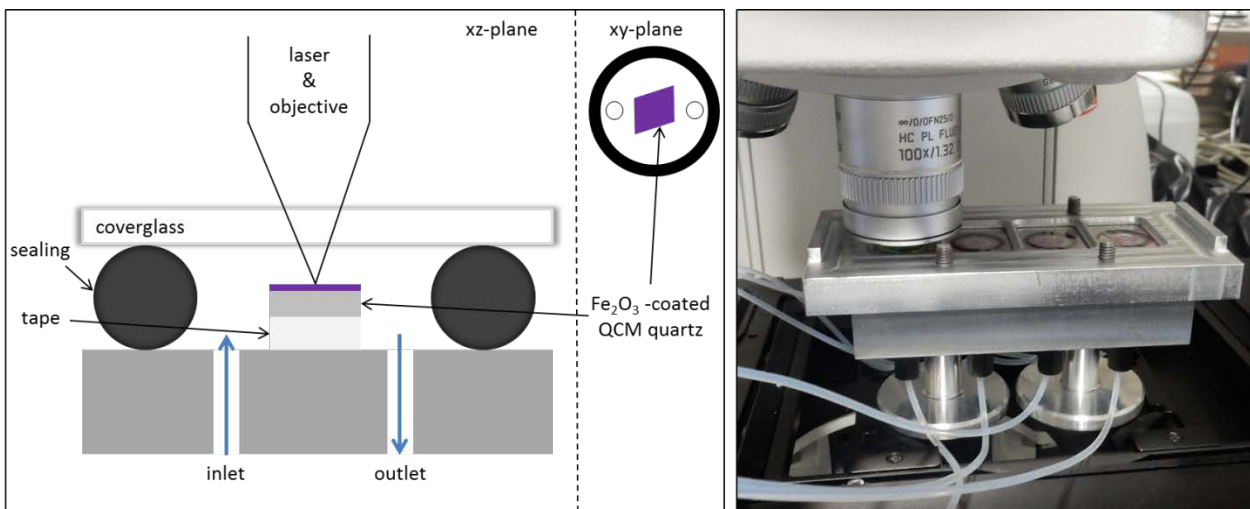


**Figure 1.** Schematic and photo of the measurement setup with flow cell under the CLSM.

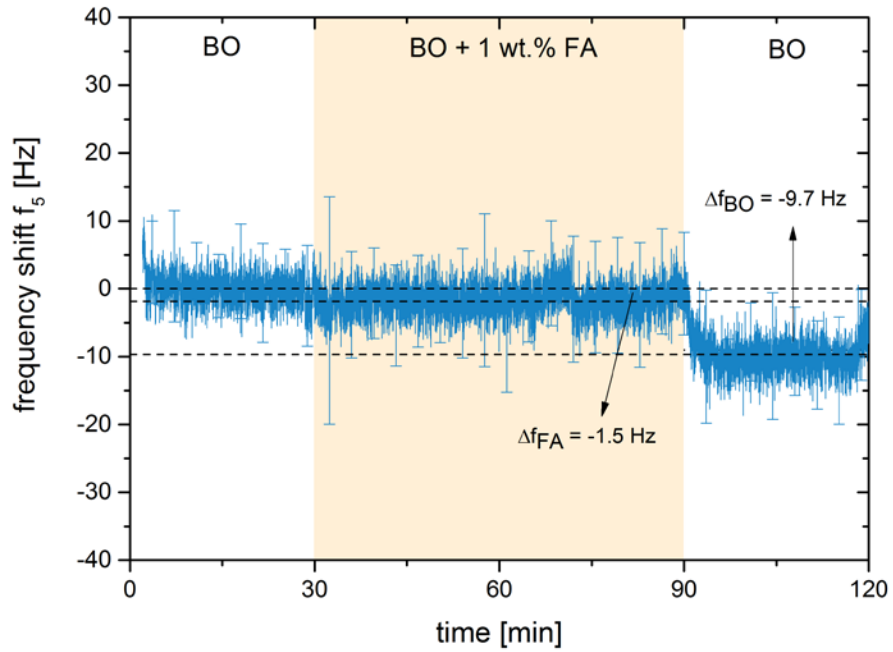


**Figure 2.** Mean value of QCM-D measurements of FA deposition from BO (frequency signal of 5<sup>th</sup> overtone); results shown for BO rinsing 0 – 30 min, BO + 1 wt.% FA rinsing 30 – 90 min and BO rinsing 90 – 120 min; error bars are standard deviation of 7 single measurements.

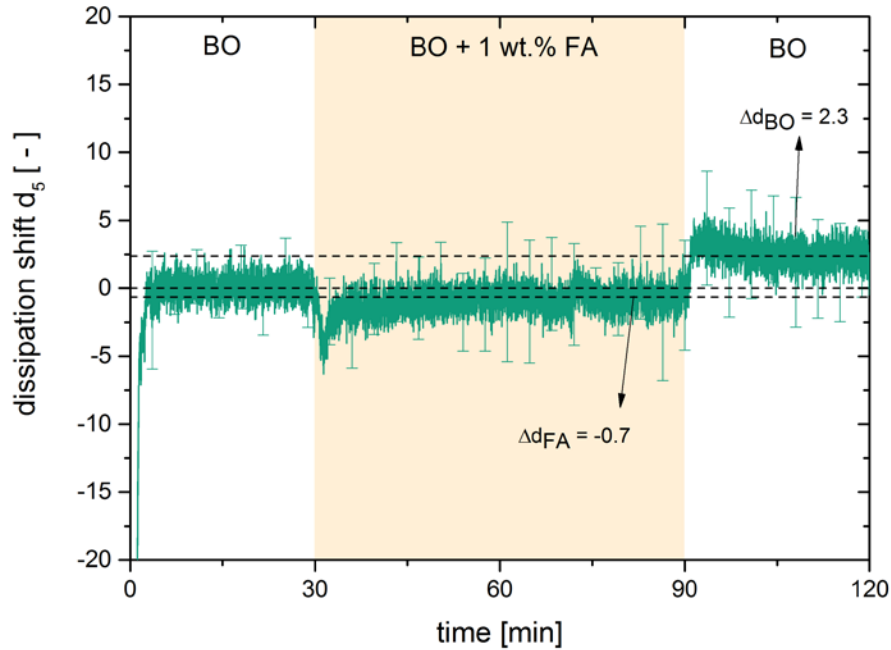


**Figure 3.** Mean value of QCM-D measurements of FA deposition from BO (dissipation signal of 5<sup>th</sup> overtone); results shown for BO rinsing 0 – 30 min, BO + 1 wt.% FA rinsing 30 – 90 min and BO rinsing 90 – 120 min; error bars are standard deviation of 7 single measurements

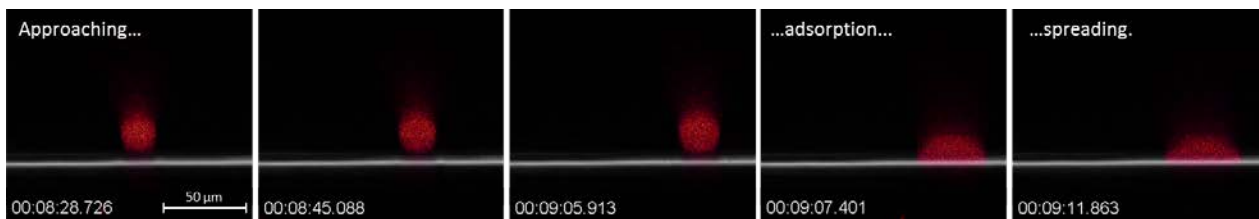


**Figure 4.** CLSM recording of the deposition of a droplet of friction modifier in xz-plane. The reflection signal at 405 nm in grey represents the Fe<sub>2</sub>O<sub>3</sub> surface, above the crystal a mixture of BO + 1 wt.% FA flows through the surface with a flow rate of approximately 140 μl/min. BO does not fluoresces (no signal), FA fluoresces at 488 nm (orange), the format of the timestamp is hh:mm:ss:mss.

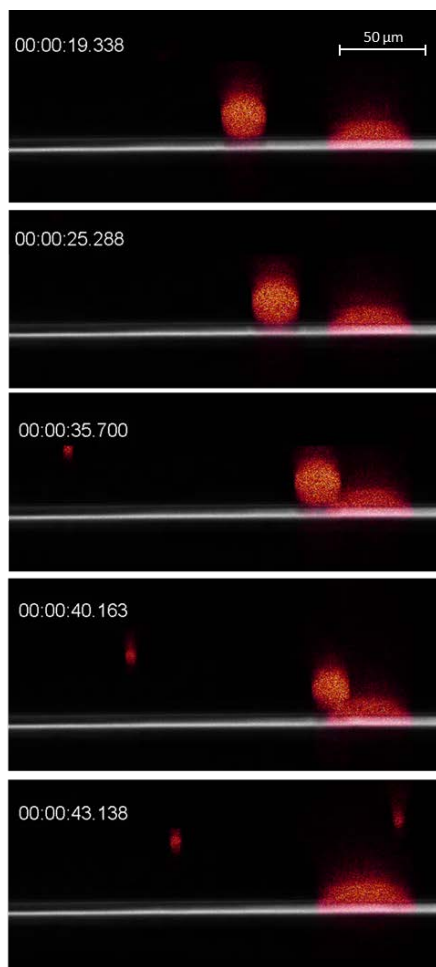


**Figure 5.** CLSM recording of two merging droplets of friction modifier in xz-plane. The reflection signal at 405 nm in grey represents the Fe<sub>2</sub>O<sub>3</sub> surface, above the crystal a mixture of BO + 1 wt.% FA flows through the surface with a flow rate of approximately 140 μl/min. BO does not fluoresces (no signal), FA fluoresces at 488 nm (orange). The format of the timestamp is hh:mm:ss:mss.

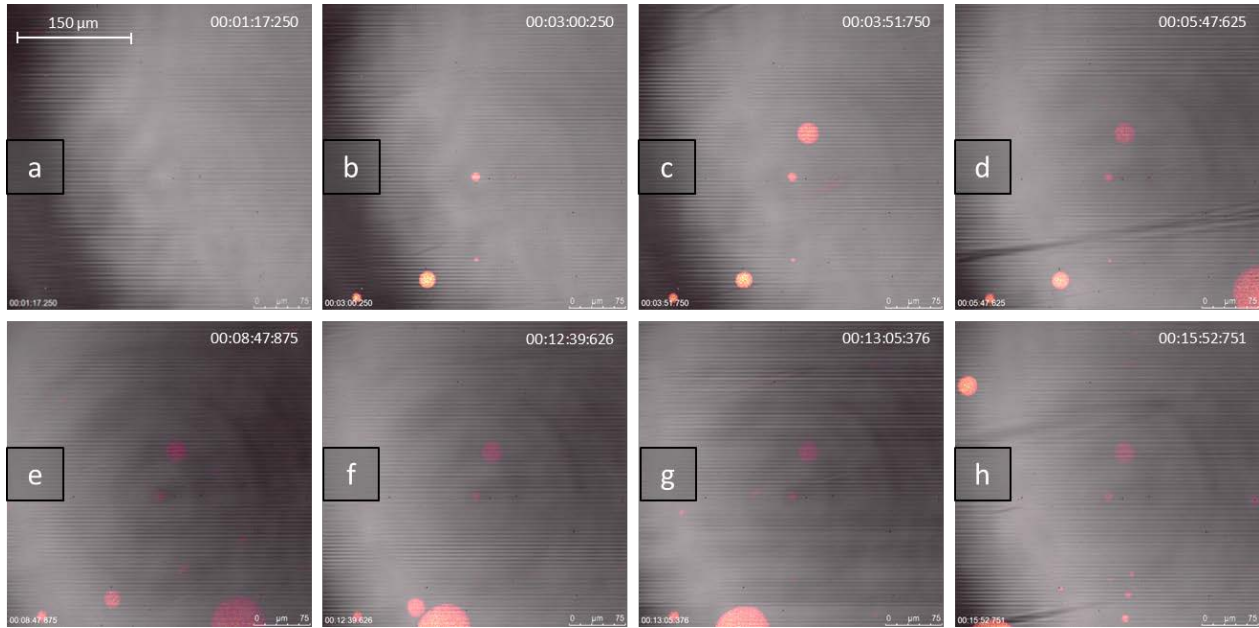


**Figure 6.** CLSM recording of the deposition of droplets of friction modifier in xy-plane. The reflection signal at 405 nm in grey represents the  $\text{Fe}_2\text{O}_3$  surface, above the crystal a mixture of BO + 1 wt.% FA flows through the surface with a flow rate of approximately 140  $\mu\text{l}/\text{min}$ . BO does not fluoresces (no signal), FA fluoresces at 488 nm (orange). The format of the timestamp is hh:mm:ss:mss.

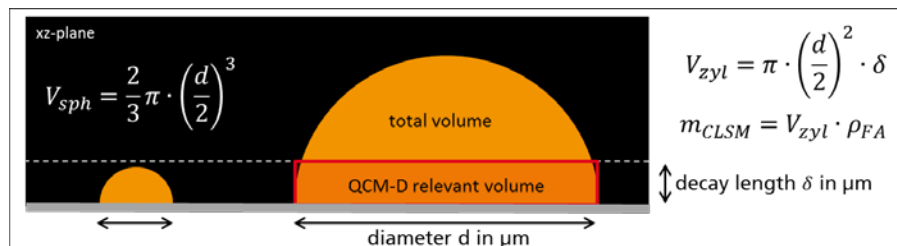


**Figure 7.** Schematic drawing of adsorbed droplet in xz-plane and used equations.

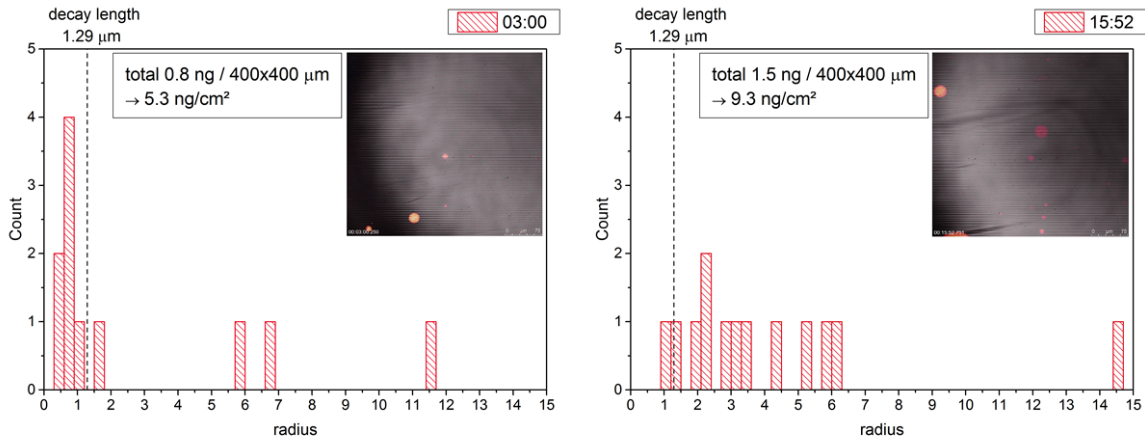


**Figure 8.** Distribution of radii for time steps 3:00 and 15:52 (compare Figure 6) during rinsing with BO + 1 wt.% FA (size of class 0.3 μm). The given masses are calculated by adding up the weight of all droplets within the area 400 x 400 μm<sup>2</sup>. Format of the timestamp is mm:ss.

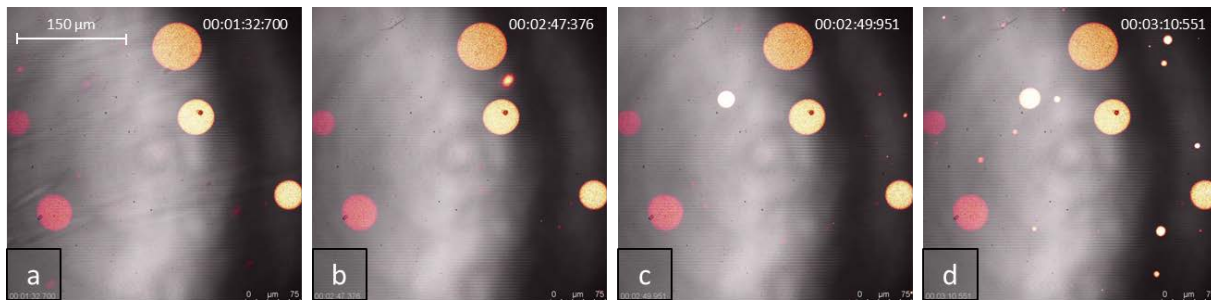


**Figure 9.** CLSM recording of the deposition of a droplet of friction modifier in xy-plane initially during rinsing with BO. The reflection signal at 405 nm in grey represents the Fe<sub>2</sub>O<sub>3</sub> surface, above the crystal a mixture of BO + 1 wt.% FA flows through the surface with a flow rate of approximately 140 μl/min. BO does not fluoresces (no signal), FA fluoresces at 488 nm (orange). The format of the timestamp is hh:mm:ss:mss.

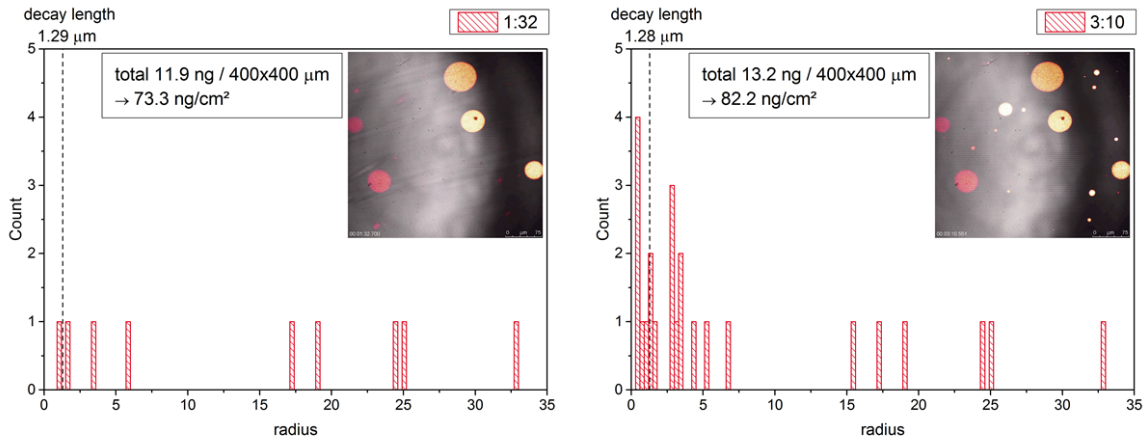


**Figure 10.** Distribution of radii for time steps 1:32 and 3:10 (compare Figure 9) during rinsing with BO (size of class 0.3  $\mu\text{m}$ ). The given masses are calculated by adding up the weight of all droplets within the area 400 x 400  $\mu\text{m}^2$ . The format of the timestamp is mm:ss.

## TABLES

**Table 2.** Physical properties of FA, BO and BO + 1 wt.% FA

	FA	BO	BO + 1 wt.% FA
kinematic viscosity [ $\text{mm}^2/\text{s}$ ]	290 (20 °C)	25.48 (55 °C)	25.94 (55°C)
density [ $\text{g}/\text{cm}^3$ ]	0.97 (20 °C)	0.84 (55 °C)	0.84 (55°C)

FA denotes the friction modifier additive, the properties of the base oil are denoted with BO

## **AUTHOR INFORMATION**

### **Corresponding Author**

\*Corresponding Author: martin.dienwiebel@kit.edu

### **Author Contributions**

The manuscript was written through contributions of all authors. All authors have given approval to the final version of the manuscript.

## **ACKNOWLEDGMENT**

The authors acknowledge the assistance by D. Bahl and S. Janson with the CLSM measurements and M. Rückel for the discussion of the results. M.D. acknowledges the Deutsche Forschungsgemeinschaft (DFG) under grant DI1494/4-1.

## **REFERENCES**

- (1) Spikes, H. Friction Modifier Additives. *Tribol Lett* 2015, 60, 119–145.
- (2) Tang, Z.; Li, S. A review of recent developments of friction modifiers for liquid lubricants (2007–present). *Current Opinion in Solid State and Materials Science* 2014, 18, 119–139.
- (3) Bowden, F. P.; Gregory, J. N.; Tabor, D. Lubrication of Metal Surfaces by Fatty Acids. *Nature* 1945, 156, 97–101.
- (4) Daniel, S. G. The adsorption on metal surfaces of long chain polar compounds from hydrocarbon solutions. *Trans. Faraday Soc.* 1951, 47, 1345–1359.
- (5) Loehle, S.; Matta, C.; Minfray, C.; Le Mogne, T.; Martin, J.-M.; Iovine, R.; Obara, Y.; Miura, R.; Miyamoto, A. Mixed Lubrication with C18 Fatty Acids: Effect of Unsaturation. *Tribology Letters* 2014, 53, 319–328.



- (6) Campen, S.; Green, J. H.; Lamb, G. D.; Spikes, H. A. In Situ Study of Model Organic Friction Modifiers Using Liquid Cell AFM; Saturated and Mono-unsaturated Carboxylic Acids. *Tribol Lett* 2015, 57, 51-71.
- (7) Kuwahara, T.; Romero, P. A.; Makowski, S.; Weihnacht, V.; Moras, G.; Moseler, M. Mechano-chemical decomposition of organic friction modifiers with multiple reactive centres induces superlubricity of ta-C. *Nature Communications* 2019, 10, 151.
- (8) Bernat, S.; Armada, S.; Espallargas, N. Friction Mechanisms by Carboxylic Acids in Aqueous Lubricants. *Tribology Letters* 2018, 66, 82-97.
- (9) Hardy, W. B.; Doubleday, I. Boundary lubrication.— The paraffin series. *Proceedings of the Royal Society of London. Series A, Containing Papers of a Mathematical and Physical Character* 1922, 100, 550–574.
- (10) Benítez, J. J.; Kopta, S.; Ogletree, D. F.; Salmeron, M. Preparation and Characterization of Self-Assembled Monolayers of Octadecylamine on Mica Using Hydrophobic Solvents. *Langmuir* 2002, 18, 6096–6100.
- (11) Zhu, Y.; Ohtani, H.; Greenfield, M. L.; Ruths, M.; Granick, S. Modification of Boundary Lubrication by Oil-Soluble Friction Modifier Additives. *Tribology Letters* 2003, 15, 127–134.
- (12) Wood, M. H.; Welbourn, R. J. L.; Charlton, T.; Zorbakhsh, A.; Casford, M. T.; Clarke, S. M. Hexadecylamine adsorption at the iron oxide-oil interface. *Langmuir* 2013, 29, 13735–13742.
- (13) Doig, M.; Camp, P. J. The structures of hexadecylamine films adsorbed on iron-oxide surfaces in dodecane and hexadecane. *Phys. Chem. Chem. Phys.* 2015, 17, 5248–5255.
- (14) Gidalevitz, D.; Huang, Z.; Rice, S. A. Urease and hexadecylamine-urease films at the air-water interface: an x-ray reflection and grazing incidence x-ray diffraction study. *Biophys J* 1999, 76, 2797–2802.

- (15) Eriksson, K. Fatty Amines as Friction Modifiers in Engine Oils: Correlating Adsorbed Amount to Friction and Wear Performance. Master Thesis, Chalmers University of Technology, Gothenburg, Schweden, 2014.
- (16) Nalam, P. C.; Pham, A.; Castillo, R. V.; Espinosa-Marzal, R. M. Adsorption Behavior and Nanotribology of Amine-Based Friction Modifiers on Steel Surfaces. *The Journal of Physical Chemistry C* 2019, 123, 13672–13680.
- (17) Jung, A. K.; Voelkel, L; Crema, S. European Patent No. EP 2321389B1
- (18) Sauerbrey, G. Verwendung von Schwingquarzen zur Wägung dünner Schichten und zur Mikrowägung. *Zeitschrift für Physik* 1959, 155, 206–222.
- (19) Qiao, X.; Zhang, X.; Tian, Y.; Meng, Y. Progresses on the theory and application of quartz crystal microbalance. *Applied Physics Reviews* 2016, 3, 31106.
- (20) Rodahl, M.; Kasemo, B. Frequency and dissipation-factor responses to localized liquid deposits on a QCM electrode. *Sensors and Actuators B: Chemical* 1996, 37, 111–116.
- (21) Evans, K. O. Quartz crystal microbalance investigation of the structure of adsorbed soybean oil and methyl oleate onto steel surface. *Thin solid films* 2010, 519, 900-905.
- (22) Reviakine, I. ; Johannsmann, D; Richter, R.P. Hearing What You Cannot See and Visualizing What You Hear: Interpreting Quartz Crystal Microbalance Data from Solvated Interfaces. *Anal. Chem.* 2011, 83, 8838–8848

Graphical Abstract

